Indolocarbazole based small molecules: an efficient hole transporting material for perovskite solar cells

ARTICLE *in* RSC ADVANCES · MAY 2015

Impact Factor: 3.84

10 AUTHORS, INCLUDING:

Iseul Lim

Hanyang University

23 PUBLICATIONS **67** CITATIONS

SEE PROFILE

Dr. Supriya Ankush Patil

Hanyang University

32 PUBLICATIONS **51** CITATIONS

SEE PROFILE

Nabeen K. Shrestha

Hanyang University

83 PUBLICATIONS **1,065** CITATIONS

SEE PROFILE

Won K Seok

Dongguk University

41 PUBLICATIONS **643** CITATIONS

SEE PROFILE

RSC Advances

PAPER

View Article Online
View Journal | View Issue

Cite this: *RSC Adv.*, 2015, **5**, 55321

Indolocarbazole based small molecules: an efficient hole transporting material for perovskite solar cells†

Iseul Lim,[a] Eun-Kyung Kim,[a] Supriya A. Patil,[a] Do Young Ahn,[a] Wonjoo Lee,[b] Nabeen K. Shrestha,*[a] Joong Kee Lee,[c] Won K. Seok,[d] Cheon-Gyu Cho[a] and Sung-Hwan Han*[a]

Received 29th May 2015
Accepted 18th June 2015

DOI: 10.1039/c5ra10148d

www.rsc.org/advances

To date, Spiro-OMeTAD, which is an expensive organic compound, has been used as the benchmark hole transporting material (HTM) in perovskite based solid state solar cells. Development of an inexpensive HTM with competitive performance to Spiro-OMeTAD is therefore significantly important for the commercialization of perovskite cells. Herein, an indolocarbazole based small molecule derivative (*C12-carbazole*) has been introduced as an environmentally stable, cost effective and highly efficient HTM. In contrast to the power conversion efficiency of 9.62% exhibited by the Spiro-OMeTAD based solid state solar cell, the *C12-carbazole* based device under the same experimental conditions has demonstrated an enhanced power conversion efficiency of 11.26%. The improved photovoltaic performance of the *C12-carbazole* based device is attributed to reduced carrier recombination by a better hole extraction ability of the *C12-carbazole*, which has demonstrated remarkably higher hole mobility compared to Spiro-OMeTAD.

1. Introduction

Solar cells have been considered the most promising green technology, and convert solar radiation directly into electricity, a highly demanded form of energy. Although silicon based solar panels, which command the largest market share, have been used mostly to harvest solar radiation and directly supply output to the public electricity grid, more efficient and cost effective materials which can substitute silicon are still highly demanded. Recently, perovskite, a crystalline organometal halide (*i.e.*, $CH_3NH_3PbX_3$), has been the main focus of research in photovoltaics with a strategy to enhance the energy conversion efficiency and reduce the material and device fabrication costs compared to silicon based solar cells.[1–13] Starting with the solar-to-electric power conversion efficiency (η) of 3.8% demonstrated by a perovskite based liquid junction device in 2009,[1] very recently a solid state prototype based on perovskite has already demonstrated breakthrough in solid state dye-sensitized solar cells with certified η of 20.1%.[14] Researchers are still pushing enormous efforts continuously to improve the cell performance further. On the basis of various results and speculations, realistic η of as high as close to the η of silicon based solar cell has been predicted from a solid-state mesoscopic solar cell based on perovskite – thus putting the material on a par with silicon.[9] Like silicon based solar cell, perovskite solar cells can also work without a hole transport material (HTM), which demonstrated a maximum η ranging from about 8 to 12%.[15–19] Nevertheless, study shows that the most efficient charge separation is obtained when using TiO_2 and HTM together. Although large number of HTMs has been introduced for a perovskite based solar cell, Spiro-OMeTAD is still demonstrating as the benchmark model for efficient HTM.[20–29] However, in addition to its relatively low hole mobility and high air/moisture sensitivity, Spiro-OMeTAD is also one of the expansive material in perovskite based solar cells. Therefore, a cost effective and efficient HTM, which can substitute Spiro-OMeTAD is highly desirable and significantly important to commercialize the perovskite based solar cells. Herein, we introduce a noble indolocarbazole based small molecule derivative (FW = 670.84) shown in Fig. 1a, and chemically can be called as 8,16-didodecyl-8,16-dihydrobenzo[*a*]benzo[6,7]indolo[2,3-*h*]carbazole (this compound is represented here as *C12-carbazole*), as an efficient HTM for perovskite based solid-state solar cells, which enables us to obtain a higher η of 11.26% as compared to 9.62% of η demonstrated by the similar device fabricated in the present work based on Spiro-OMeTAD

[a]*Department of Chemistry, Hanyang University 17, Haengdang-dong, Seongdong-gu, Seoul, 133-791 Korea. E-mail: nabeenkshrestha@hotmail.com; shhan@hanyang.ac.kr*
[b]*Department of Defense Ammunitions, Daeduk College, Daejeon, Korea*
[c]*Advanced Energy Materials Processing Laboratory, Center for Energy Convergence Research, Green City Technology Institute, Korea Institute of Science and Technology (KIST), Seoul, 130-650 Korea*
[d]*Dongguk Univ-Seoul, Department of Chemistry, Seoul, 100-715 Korea*

† Electronic supplementary information (ESI) available. See DOI: 10.1039/c5ra10148d

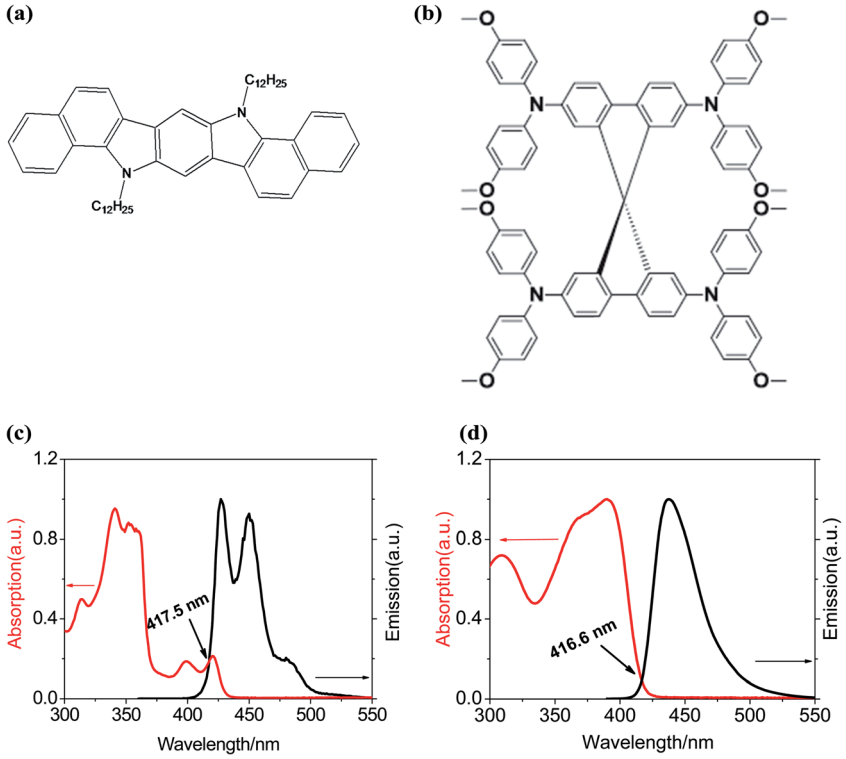

Fig. 1 Molecular structure of (a) *C12-carbazole*, and (b) Spiro-OMeTAD. Normalized UV/Visible and PL emission spectra of 9 mM solution of (c) *C12-carbazole*, and (d) Spiro-OMeTAD in chlorobenzene.

HTM. It should be worthwhile to mention that η of the perovskite based solid-state device has been suffered from large variations in device performance and reproducibility.[14] In addition, generally η higher than the average value of 12 $\pm$ 2% (ref. 13) has been successfully demonstrated only by world leading research groups on perovskite based solar cells. Nevertheless, η achieved by the *C12-carbazole* based device of the present work is closer to the above mentioned average efficiency of the similar device based on Spiro-OMeTAD HTM, but the efficiency is still higher than that of the Spiro-OMeTAD HTM based device constructed under similar experimental conditions in our laboratory.

2. Experimental details

2.1 Materials

All chemicals were of analytical grade, and they were used as obtained from the suppliers without further purification. *C12-carbazole* was synthesized as described in our previous work.[30] Briefly, Cu(I)-catalyzed coupling reaction between 4-diiodobenzene and benzyl carbazate was carried out to obtain benzyl 1,1′-(1,4-phenylene)bis(hydrazinecarboxylate). A double Fischer indolization reaction was carried out by mixing and refluxing the above reaction product with α-tetralone and 0.4 M H_2SO_4 in EtOAc. Thus, linear and angular inseparable 3 to 1 mixture of *N*,*N*′-bis-Cbz indolocarbazole was obtained, which was then aromatized using 2,3-dichloro-5,6-dicyano-1,4-benzoquinone. The mixture of linear and angular products from aromatization was separated by virtue of their solubility differences. Recrystallization of the aromatized product from EtOAc provided dibenzyl benzo[*a*]benzo[6,7]indolo[2,3-*h*] carbazole-8,16-dicarboxylate, which upon unmasking the two Cbz groups, and subsequent alkylation with dodecyl bromide yielded *C12-carbazole* (90% yield). The formation of *C12-carbazole* was confirmed using ^{1}H, ^{13}C NMR and mass spectroscopy.

2.2 Device fabrication

Solid state perovskite solar cells were fabricated using the method reported previously.[31,32] The method is described briefly here. Approximately 60 nm of TiO_2 blocking layer was coated on patterned and cleaned fluorine-doped tin oxide-coated (FTO) glasses (Pilkington, 7 Ω sq^{-1}) by spinning 0.15 M titanium diisopropoxide bis(acetylacetonate) (75%, Sigma-Aldrich) prepared in anhydrrous 1-butanol (99.9%, Alfa Aesar) solution at 3000 rpm followed by heat treatment at 125 °C for 5 min. The procedure was repeated for 3 cycles, and finally the spin-coated FTO glasses were heated at 500 °C for 20 min.

An approximately 0.6 μm thick mesoporous layer of TiO_2 was deposited onto the blocking layer coated FTO glasses by spin coating using diluted TiO_2 paste (TTP-20N, ENB Korea) in isopropyl alcohol (IPA, ≥99.7%) (TiO_2 : IPA ratio was 1 : 3.5 by wt) at 4000 rpm. The layers were then sintered at 450 °C in air for 1 h. The mesoporous TiO_2 film coated FTO glasses were immersed in 0.02 M aqueous $TiCl_4$ (>98%, Sigma-Aldrich) solution at 70 °C for 60 min. After washing with deionized water and drying, the film was heated at 500 °C for 30 min.

1 M solution of PbI_2 solution was prepared by dissolving 461 mg PbI_2 (99%, Aldrich) in 1 mL DMF, (99.8%, Sigma-Aldrich) under stirring at 60 °C. 20 μL of the PbI_2 solution was spin-coated on to the mesoporous TiO_2 film at 3000 rpm for 5 s followed by repeating the cycle at 6000 rpm for 5 s (without loading time). The film was then dried at 40 °C for 3 min, and again at 100 °C for 5 min. After cooling the film down to room temperature, 200 μL of 0.063 M CH_3NH_3I perovskite solution in 2-propanol was loaded on to the PbI_2-coated TiO_2 film for 20 s, which was then spun at 4000 rpm for 20 s and dried at 100 °C for 30 min.

To use 2,2′,7,7′-tetrakis(*N*,*N*-di-*p*-methoxyphenylamine)-9,9-spirobifluorene (Spiro-OMeTAD) as HTM,[31] 20 μL of Spiro-OMeTAD solution (which was prepared by dissolving 72.3 mg of Spiro-MeOTAD (SHT-263, MERCK) in 1 mL of anhydrous chlorobenzene (99.8%, Sigma-Aldrich)), to which already 28.8 μL of 4-*tert*-butyl pyridine (96%, Sigma-Aldrich) and 17.5 μL of lithium bis(trifluoromethanesulfonyl)imide (Li-TFSI, Alfa Aesar from 98%, solution containing 520 mg Li-TSFI in 1 mL acetonitrile was added) was spin-coated on to the $CH_3NH_3PbI_3$ perovskite layer coated TiO_2 film at 3000 rpm for 30 s.

Similarly, to use *C12-carbazole* as HTM,[32] 70 mL 4 wt% of *C12-carbazole* in chlorobenzene solution mixed with 4-*tert*-butyl pyridine and Li-TFSI was loaded on to the $CH_3NH_3PbI_3$ perovskite layer coated TiO_2 film (area 2.5 × 2.5 cm^{-2}) for 1 minute, and spun at 3000 rpm for 30 s. The above *C12-carbazole* HTM solution for spin-coating was prepared as follows. 4-*tert*-Butyl pyridine was added to 4 wt% *C12-carbazole* solution with a volume to mass ratio of 1 : 26 μL mg^{-1}. To this mixture, Li-TFSI (pre-dissolved in acetonitrile at 170 mg mL^{-1}) was added at 1 : 12 μL mg^{-1} of Li-TFSI solution: *C12-carbazole*. After spin coating, the film was dried overnight in Ar-atmosphere inside a glove box.

Finally, ~80 nm of gold was thermally evaporated on the HTM-coated films.

3. Results and discussion

C12-carbazole (Fig. 1a) was synthesized as a yellow solid with M_w = 670.84 g mol^{-1}, and its chemical composition was confirmed as described in our previous work.[30] Based on the molar mass, *C12-carbazole* is nearly two times smaller than Spiro-OMeTAD (Fig. 1b, M_w = 1225 g mol^{-1}) molecule (Fig. 1b), and as compared to the expensive Spiro-OMeTAD, the total cost of synthesis of *C12-carbazole* is relatively cheaper. In addition, as compared to Spiro-OMeTAD, *C12-carbazole* is relatively hydrophobic, and is therefore environmentally more stable. As a result, previously we could fabricate Field-Effect Transistors based on *C12-carbazole* nanowires at room temperature and pressure on an experimental desk outside a glove box.[30] The device under these open laboratory conditions did not show performance degradation up to 30 days. This report reveals that *C12-carbazole* is relatively less sensitive to moisture and air, and hence it is environmentally more stable. This finding suggests that *C12-carbazole* can be handled more easily while fabricating the devices. On the other hand, *C12-carbazole* has demonstrated remarkably high carrier mobility. The hole mobility of a single crystalline nanowire of *C12-carbazole* has been measured previously[30] as 1.5 cm^2 V^{-1} s^{-1}, which is significantly higher than that of Spiro-OMeTAD (5.31 × 10^{-5} cm^2 V^{-1} s^{-1}).[25] Considering the advantage of these perspectives of the materials, *C12-carbazole* is investigated in the present work as a potential HTM for solid state perovskite solar cells, and comparatively studied with the Spiro-OMeTAD based cells.

The optical absorption/emission spectra of *C12-carbazole* and Spiro-OMeTAD are shown in Fig. 1c and d, respectively. Fig. 1c shows the strong absorption of UV light at about 341 nm and a very weak absorption of visible light at about 421 nm. Such a weak absorption of visible light suggests that *C12-carbazole* would not interfere the penetration of visible light reaching to the sensitizer inside the mesoporous layer structure of the device. Meanwhile, it should be noted that the emission spectrum shown in Fig. 1c has intersected the absorption spectrum at 417.5 nm, which suggests the optical band gap of *C12-carbazole* equals to 2.97 eV. This value is close to those of Spiro-OMeTAD as shown in Fig. 1d, and X51 – a carbazole based HTMs[25] (see Fig. S1†) as summarized in Table 1. Thus, these three HTMs have more or less similar energy gap. The ground state oxidation of the HTMs, which corresponds to the highest occupied molecular orbital (HOMO) level, should be suitably situated in order to keep the optimized balance between hole-transfer yield and open-circuit voltage (V_{oc}) of the device.[33,34] In the present work, the ground state oxidation of *C12-carbazole* is determined using cyclic voltammetry. Fig. S2† shows the cyclic voltamogram of *C12-carbazole* film in acetonitrile containing 0.1 M tetrabutyl ammonium tetrafluoroborate as a supporting electrolyte. From the onset potential of the anodic branch of the voltamogram, the ground state oxidation is estimated at 0.79 V *vs.* NHE, which reveals the HOMO energy level of −5.29 eV below vacuum level. Although, this HOMO level is little lower than those of Spiro-OMeTAD, X51 and P3HT, based on the HOMO energy level of the $CH_3NH_3PbI_3$ perovskite sensitizer (−5.46 eV (ref. 34)), the 0.17 eV over potential is large enough driving force for the complete hole transportation (Fig. S3†), and thereby a complete regeneration of the oxidized dye can be ensured.[33,34] Apart from the HOMO level, hole mobility of the material is another key factor to be considered while designing a new HTM. In the present work, hole mobility of *C12-carbazole* was estimated by constructing an organic thin film transistor, and measuring drain current–gate voltage transfer curves (Fig. S4†) as reported previously.[30] Fig. S5a† shows the SEM top view of the spin-coated film on, which exhibits a thin fused mass of *C12-carbazole* in the film, and being significantly smaller than Spiro-OMeTAD and X51, the *C12-carbazole* can easily contact with the $CH_3NH_3PbI_3$. This indicates that *C12-carbazole* can easily infiltrate and the infiltrated mass can make interconnections together with a thin over layer of *C12-carbazole* on the top of the mesoporous structures of the device (Fig. S5b†), which is highly desirable and significantly important to extract holes efficiently.[7,12] The measured hole mobility of the *C12-carbazole* film have been comparatively summarized to those of the reported values of Spiro-OMeTAD and X51 in Table 1. The hole mobility of the *C12-carbazole* film is less than that for a single crystalline

Table 1 Optoelectronic properties of various HTMs

HTMs	*C12-carbazole*	Spiro-OMeTAD[a]	X51[b]
λ_{abs} (nm)	341(max); 352; 399; 421	356; 386(max)	307(max); 365
λ_{em} (nm)	427(max); 450	423	469
Band gap (nm)	2.97	2.98	2.93
HOMO (eV)	−5.29	−5.13	−5.14
Hole mobility ($cm^2\ V^{-1}\ s^{-1}$)	[c]1.5; [d]5.1×10^{-2}	5.31×10^{-5}	1.51×10^{-4}

[a] Data from ref. 22. [b] Data from ref. 22. [c] Single crystal nanowire data from ref. 27. [d] Spin-coated film of this work.

C12-carbazole nanowire, which we reported earlier.[30] The higher hole mobility of the *C12-carbazole* in nanowire architecture could be due to the unidirectional charge transportation. Nevertheless, the hole mobility of the spin-coated *C12-carbazole* film is still remarkably higher, which is higher by three and two order of magnitude as compared to those of Spiro-OMeTAD and X51, respectively.

Based on the above optoelectronic properties, *C12-carbazole* has been investigated as the potentially efficient HTM in a perovskite based solid-state solar cell, and compared with the similar cell based on Spiro-OMeTAD HTM. For this, we constructed a solid-state mesoscopic device with the following configuration: compact TiO_2/400 nm mesoporous TiO_2/$CH_3NH_3PbI_3$/HTM-Li-TFSI/Au. The detail configuration of the device can be viewed at the SEM cross-sectional image of the cell shown in Fig. 2. The devices were constructed using the standard method as used for the Spiro-OMeTAD based cell without further any optimizations. The details about the construction of the device have been described in the ESI,† and the details on the characterization of the cells are discussed below.

Fig. 3 shows the photoluminescence (PL) emission spectra of the $CH_3NH_3PbI_3$ sensitized TiO_2 film on a glass substrate before and after addition of HTMs. The emission spectra reveal that the intense fluorescence exhibited by the $CH_3NH_3PbI_3$–TiO_2 film has been quenched quantitatively after the addition of both HTMs. The similar degree of PL quenching suggests that both HTMs establish an easy electron transfer path from $CH_3NH_3PbI_3$ to TiO_2 by extracting the holes efficiently, and thereby making an efficient charge separation. Thus, a highly competitive photovoltaic performance of the devices based on these two HTMs can be expected. Fig. 4a shows the typical characteristic current–voltage (*J–V*) curves obtained from the best performing devices of the present work, and the detail photovoltaic parameters obtained from the *J–V* curves are tabulated in Table 2. It is important to note that, in contrast to η of 9.62% exhibited by the Spiro-OMeTAD based cell, the *C12-carbazole* based device has demonstrated a better photovoltaic performance with a η of 11.26%. As evident in Fig. 4a, the short-circuit current densities (J_{sc}) of the devices based on both HTMs are similar. Therefore, their contribution to η should also be similar, which is also supported by the similar incident-photon-to-current efficiency (IPCE) of the both devices (Fig. 4b).

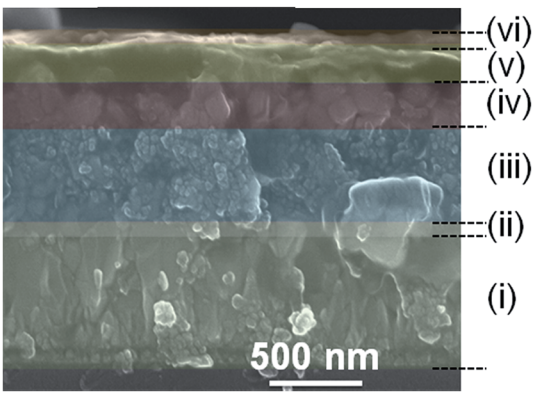

Fig. 2 SEM cross-sectional view of the perovskite cell. (i) 600 nm FTO, (ii) 60 nm compact TiO_2, (iii) 400 nm mesoporous TiO_2, (iv) 180 nm perovskite over layer, (v) 140 nm *C12-carbazole* over layer, and (vi) 80 nm gold film.

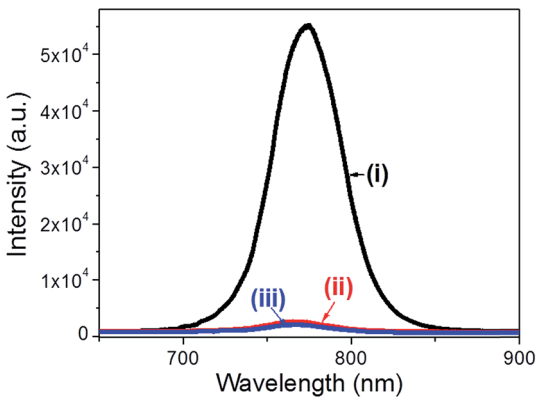

Fig. 3 PL emission spectra of (i) TiO_2–$CH_3NH_3PbI_3$, (ii) TiO_2–$CH_3NH_3PbI_3$–*C12-carbazole*, and (iii) TiO_2–$CH_3NH_3PbI_3$–Spiro-OMeTAD films.

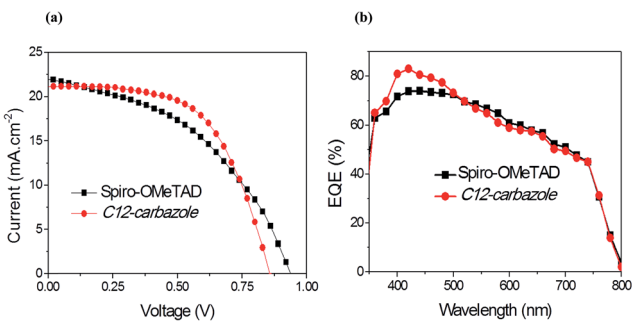

Fig. 4 (a) *J–V* curves, and (b) incident-photon-to-current efficiency (IPCE) spectra of the perovskite cells with two different HTMs.

Table 2 Photovoltaic parameters obtained from J–V curves of the perovskite cells based on two different HTMs

HTMs	V_{oc} (V)	J_{sc} (mA cm^{-2})	FF	Eff. (%)
C12-carbazole	0.86	21.13	0.62	11.26
Spiro-OMeTAD	0.93	21.97	0.47	9.62

Based on the J–V curves in Fig. 4a, the better η of the *C12-carbazole* based cell can be undoubtedly ascribed to the better fill factor (FF) of the device, which is mainly controlled by the carrier recombination of the devices. In the present work, the degree of carrier recombination of the two devices with different HTMs was investigated by investigating the photovoltage decay kinetics. As expected, relatively sluggish photovoltage decay kinetic of the *C12-carbazole* HTM based device can be observed in Fig. 5. This suggests an improved charge separation of the device from the better hole extraction ability of the *C12-carbazole*, and thereby a better photovoltaic performance of the device shown in Fig. 4a and Table 2 can be assured. In addition to the better power conversion efficiency, a fairly good reproducibility of the device fabrication and performance, while examining a number of devices fabricated with *C12-carbazole* HTM, was also obtained (Fig. S6 and Table S1†). In this case, η of as low as 8.73% was obtained, which is within the acceptable range of deviation. It should be also noted that the present *C12-carbazole* based device has demonstrated a better photovoltaic performance than that of the previously reported X51 (which is also a carbazole based small molecule) HTM[25] based device (Table 2).

On the other hand, apart from Spiro-OMeTAD as a model for small molecule HTM, various polymeric hole conductors such as P3HT, PTAA, and PANI have also been used in perovskite solar cells.[29,35–37] Among them, P3HT is often used as model polymeric HTM in solar cells owing to their suitable carrier mobility, conductivity and compatible HOMO energy level to the light harvesting sensitizers (Table S2†). Therefore, it would be worthy to compare the photovoltaic performance of a perovskite solar cell based on P3HT HTM. When a perovskite based solid state solar cell similar to the one described above but with P3HT as HTM was constructed in the present study, the device demonstrated a η of 7.25% (Fig. S7†). As compared to *C12-carbazole* and Spiro-OMeTAD based cells, the poor photovoltaic performance of the P3HT based device under similar experimental conditions could be due to the poor infiltration of the P3HT into the mesoporous structure of the device owing to its larger molecular size. This is one of the reasons for the great attraction of researchers on development of small molecular HTMs.

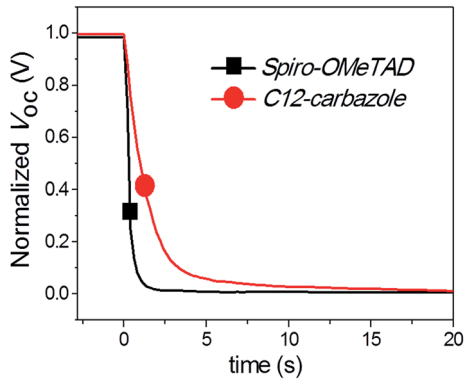

Fig. 5 Photovoltage decay kinetics after stopping illumination of the perovskite solar cell based on two different HTMs.

4. Conclusions

Based on the results of the present work, *C12-carbazole* can be considered as a frugal, efficient and providently competitive HTM as compared to the Spiro-OMeTAD, which is the benchmark HTM in perovskite based solar cells. In addition, as compared to X51 and P3HT, the present study demonstrates *C12-carbazole* as an efficient HTM for the perovskite based solid state solar cell. The photovoltage decay kinetic study reveals that as compared to the Spiro-OMeTAD HTM based device, an improved charge separation of the *C12-carbazole* HTM based device is obtained from the better hole extraction ability of the *C12-carbazole*, and thereby a better photovoltaic performance of the device can be obtained. Works to further improve the performance of the *C12-carbazole* HTM based perovskite solar cell is underway.

Acknowledgements

This research was supported by the KIST Institutional Program (2E23964) and by Basic Science Research Program through the National Research Foundation of Korea (NRF) funded by the Ministry of Education (2013009768). One of authors (Won K. Seok) appreciates support from research program of Dongguk University 2014, and N. K. Shrestha acknowledges The Korean Federation of Science and Technology Societies for the support under Brain Pool program.

References

1 A. Kojima, K. Teshima, Y. Shirai and T. Miyasaka, Organometal Halide Perovskites as Visible-Light Sensitizers for Photovoltaic Cells, *J. Am. Chem. Soc.*, 2009, **131**, 6050–6051.

2 J. H. Im, C. R. Lee, J. W. Lee, S. W. Park and N. G. Park, 6.5% Efficient Perovskite Quantum-Dot-Sensitized Solar Cell, *Nanoscale*, 2011, **3**, 4088–4093.

3 H. S. Kim, C. R. Lee, J. H. Im, K. B. Lee, T. Moehl, A. Marchioro, S. J. Moon, R. Humphry-Baker, J. H. Yum, J. E. Moser, M. Grätzel and N. G. Park, Lead Iodide Perovskite Sensitized All-Solid-State Submicron Thin Film Mesoscopic Solar Cell with Efficiency Exceeding 9%, *Sci. Rep.*, 2012, **2**, 591–597.

4 M. M. Lee, J. Teuscher, T. Miyasaka, T. N. Murakami and H. J. Snaith, Efficient Hybrid Solar Cells Based on Meso-Superstructured Organometal Halide Perovskites, *Science*, 2012, **338**, 643–647.

5 L. Etgar, P. Gao, Z. Xue, Q. Peng, A. K. Chandiran, B. Liu, M. K. Nazeeruddin and M. Grätzel, Mesoscopic $CH_3NH_3PbI_3/TiO_2$ Heterojunction Solar Cells, *J. Am. Chem. Soc.*, 2012, **134**, 17396–17399.

6 M. Liu, M. B. Johnston and H. J. Snaith, Efficient Planar Heterojunction Perovskite Solar Cells by Vapour Deposition, *Nature*, 2013, **501**, 395–398.

7 J. Burschka, N. Pellet, S.-J. Moon, R. Humphry-Baker, P. Gao, M. K. Nazeeruddin and M. Gratzel, Sequential Deposition as a Route to High-Performance Perovskite-Sensitized Solar Cells, *Nature*, 2013, **499**, 316–319.

8 J. H. Noh, S. H. Im, J. H. Heo, T. N. Mandal and S. I. Seok, Chemical Management for Colorful, Efficient, and Stable Inorganic-Organic Hybrid Nanostructured Solar Cells, *Nano Lett.*, 2013, **13**, 1764–1769.

9 N.-G. Park, Organometal Perovskite Light Absorbers Toward a 20% Efficiency Low-Cost Solid-State Mesoscopic Solar Cell., *J. Phys. Chem. Lett.*, 2013, **4**, 2423–2429.

10 D. Liu and T. L. Kelly, Perovskite Solar Cells with a Planar Heterojunction Structure Prepared Using Room-Temperature Solution Processing Techniques, *Nat. Photonics*, 2014, **8**, 133–138.

11 K. Wojciechowski, M. Saliba, T. Leijtens, A. Abatea and H. J. Snaith, Sub-150 °C Processed Meso-Superstructured Perovskite Solar Cells with Enhanced Efficiency, *Energy Environ. Sci.*, 2014, **7**, 1142–1147.

12 S. Kazim, M. K. Nazeeruddin, M. Grätzel and S. Ahmad, Perovskite as Light Harvester: A Game Changer in Photovoltaics, *Angew. Chem., Int. Ed.*, 2014, **53**, 2812–2824.

13 J.-H. Im, I.-H. Jang, N. Pellet, M. Grätzel and N.-G. Park, Growth of $CH_3NH_3PbI_3$ Cuboids with Controlled Size for High-Efficiency Perovskite Solar Cells, *Nat. Nanotechnol.*, 2014, **9**, 927–932.

14 http://www.nrel.gov/ncpv/images/efficiency_chart.jpg.

15 W. A. Laban and L. Etgar, Depleted Hole Conductor-Free Lead Halide Iodide Heterojunction Solar Cells, *Energy Environ. Sci.*, 2013, **6**, 3249–3253.

16 A. Mei, X. Li, L. Liu, Z. Ku, T. Liu, Y. Rong, M. Xu, M. Hu, J. Chen, Y. Yang, M. Grätzel and H. Han, A Hole-Conductor-Free, Fully Printable Mesoscopic Perovskite Solar Cell with High Stability, *Science*, 2014, **345**, 295–298.

17 Y. Xiao, G. Han, Y. Li, M. Li, Y. Chang and J. Wu, Preparation of High Performance Perovskite-Sensitized Nanoporous Titanium Dioxide Photoanodes by *in situ* Method for Use in Perovskite Solar Cells, *J. Mater. Chem. A*, 2014, **2**, 16531–16537.

18 Y. Xiao, G. Han, Y. Li, M. Li and J. Wu, Electrospun Lead-Doped Titanium Dioxide Nanofibers and The *in situ* Preparation of Perovskite-Sensitized Photoanodes for Use in High Performance Perovskite Solar Cells, *J. Mater. Chem. A*, 2014, **2**, 16856–16862.

19 Y. Xiao, G. Han, Y. Chang, Y. Zhang, Y. Li and M. Li, Investigation of Perovskite-Sensitized Nanoporous Titanium Dioxide Photoanodes with Different Thicknesses in Perovskite Solar Cells, *J. Power Sources*, 2015, **286**, 118–123.

20 B. Cai, Y. D. Xing, Z. Yang, W. H. Zhang and J. S. Qiu, High Performance Hybrid Solar Cells Sensitized by Organolead Halide Perovskites, *Energy Environ. Sci.*, 2013, **6**, 1480–1485.

21 J. H. Heo, S. H. Im, J. H. Noh, T. N. Mandal, C.-S. Lim, J. A. Chang, Y. H. Lee, H.-J. Kim, A. Sarkar, M. K. Nazeeruddin, M. Grätzel and S. I. Seok, Efficient Inorganic–Organic Hybrid Heterojunction Solar Cells Containing Perovskite Compound and Polymeric Hole Conductors, *Nat. Photonics*, 2013, **7**, 486–491.

22 D. Bi, L. Yang, G. Boschloo, A. Hagfeldt and E. M. J. Johansson, Effect of Different Hole Transport Materials on Recombination in $CH_3NH_3PbI_3$ Perovskite-Sensitized Mesoscopic Solar Cells, *J. Phys. Chem. Lett.*, 2013, **4**, 532–1536.

23 N. J. Jeon, J. Lee, J. H. Noh, M. K. Nazeeruddin, M. Grätzel and S. I. Seok, Efficient inorganic–organic hybrid perovskite solar cells based on pyrene arylamine derivatives as hole-transporting materials, *J. Am. Chem. Soc.*, 2013, **135**, 19087–19090.

24 H. Li, K. Fu, A. Hagfeldt, M. Grätzel, S. G. Mhaisalkar and A. C. Grimsdale, A Simple 3,4-Ethylenedioxythiophene Based Hole-Transporting Material for Perovskite Solar Cells, *Angew. Chem., Int. Ed.*, 2014, **53**, 4085–4088.

25 B. Xu, E. Sheibani, P. Liu, J. Zhang, H. Tian, N. Vlachopoulos, G. Boschloo, L. Kloo, A. Hagfeldt and L. Sun, Carbazole-Based Hole-Transport Materials for Efficient Solid-State Dye-Sensitized Solar Cells and Perovskite Solar Cells, *Adv. Mater.*, 2014, **26**, 6629–6634.

26 J. A. Christians, R. C. M. Fung and P. V. Kamat, An Inorganic Hole Conductor for Organo-Lead Halide Perovskite Solar Cells. Improved Hole Conductivity with Copper Iodide, *J. Am. Chem. Soc.*, 2014, **136**, 758–764.

27 D. S. Sung, M. S. Kang, I. T. Choi, H. M. Kim, H. Kim, M. Hong, H. K. Kim and W. I. Lee, 14.8% Perovskite Solar Cells Employing Carbazole Derivatives as Hole Transporting Materials, *Chem. Commun.*, 2014, **50**, 14161–14163.

28 A. Krishna, D. Sabba, H. Li, J. Yin, P. P. Boix, C. Soci, S. G. Mhaisalkar and A. C. Grimsdale, Novel Hole Transporting Materials Based on Triptycene Core for High Efficiency Mesoscopic Perovskite Solar Cells, *Chem. Sci.*, 2014, **5**, 2702–2709.

29 J. Liu, Y. Wu, C. Qin, X. Yang, T. Yasuda, A. Islam, K. Zhang, W. Peng, W. Chena and L. Han, A Dopant-Free Hole-Transporting Material for Efficient and Stable Perovskite Solar Cells, *Energy Environ. Sci.*, 2014, **7**, 2963–2967.

30 K. S. Park, S. M. Salunkhe, I. Lim, C.-G. Cho, S. H. Han and M. M. Sung, High-Performance Air-Stable Single-Crystal Organic Nanowires Based on a New Indolocarbazole Derivative for Field-Effect Transistors, *Adv. Mater.*, 2013, **25**, 3351–3356.

31 J. W. Lee, D. J. Seol, A. N. Cho and N. G. Park, High-Efficiency Perovskite Solar Cells Based on the Black Polymorph of $HC(NH_2)_2PbI_3$, *Adv. Mater.*, 2014, **26**, 4991–4998.

32 I. K. Ding, N. Tétreault, J. Brillet, B. E. Hardin, E. H. Smith, S. J. Rosenthal, F. Sauvage, M. Grätzel and M. D. McGehee, Pore-Filling of Spiro-OMeTAD in Solid-State Dye Sensitized Solar Cells: Quantification, Mechanism, and Consequences for Device Performance, *Adv. Funct. Mater.*, 2009, **19**, 2431–2436.

33 B. E. Hardin, H. J. Snaith and M. D. McGehee, The Renaissance of Dye-Sensitized Solar Cells, *Nat. Photonics*, 2012, **6**, 162–169.

34 S. Ryu, J. H. Noh, N. J. Jeon, Y. C. Kim, W. S. Yang, J. Seo and S. I. Seok, Voltage Output of Efficient Perovskite Solar Cells with High Open-Circuit Voltage and Fill Factor, *Energy Environ. Sci.*, 2014, **7**, 2614–2618.

35 J. H. Heo, S. H. Im, J. H. Noh, T. N. Mandal, C.-S. Lim, J. A. Chang, Y. H. Lee, H.-J. Kim, A. Sarkar, M. K. Nazeeruddin, M. Grätzel and S. I. Seok, Efficient Inorganic–Organic Hybrid Heterojunction Solar Cells Containing Perovskite Compound and Polymeric Hole Conductors, *Nat. Photonics*, 2013, **7**, 486–491.

36 F. Di Giacomo, S. Razza, F. Matteocci, A. D'Epifanio, S. Licoccia, T. M. Brown and A. Di Carlo, High Efficiency CH3NH3PbI(3−*x*)Cl*x* Perovskite Solar Cells with Poly(3-hexylthiophene) Hole Transport Layer, *J. Power Sources*, 2014, **251**, 152–156.

37 Y. Xiao, G. Han, Y. Chang, H. Zhou, M. Li and Y. Li, An All-Solid-State Perovskite-Sensitized Solar Cell Based on The Dual Function Polyaniline as The Sensitizer and p-type Hole-Transporting Material, *J. Power Sources*, 2014, **267**, 1–8.